Arthritis & Rheumatology
Vol. 72, No. 10, October 2020, pp 1749–1758
DOI 10.1002/art.41314

American College of Rheumatology
Empowering Rheumatology Professionals

Intraarticular Adeno-Associated Virus Serotype AAV-PHP.S–Mediated Chemogenetic Targeting of Knee-Innervating Dorsal Root Ganglion Neurons Alleviates Inflammatory Pain in Mice

Sampurna Chakrabarti,[1] Luke A. Pattison,[1] Balint Doleschall,[2] Rebecca H. Rickman,[1] Helen Blake,[1] Gerard Callejo,[1] Paul A. Heppenstall,[2] and Ewan St. John Smith[1]

Objective. Joint pain is the major clinical symptom of arthritis that affects millions of people. Controlling the excitability of knee-innervating dorsal root ganglion (DRG) neurons (knee neurons) could potentially provide pain relief. We undertook this study to evaluate whether the newly engineered adeno-associated virus (AAV) serotype, AAV-PHP.S, can deliver functional artificial receptors to control knee neuron excitability following intraarticular knee injection.

Methods. The AAV-PHP.S virus, packaged with dTomato fluorescent protein and either excitatory (G_q) or inhibitory (G_i) designer receptors exclusively activated by designer drugs (DREADDs), was injected into the knee joints of adult mice. Labeling of DRG neurons with AAV-PHP.S from the knee was evaluated using immunohistochemistry. The functionality of G_q- and G_i-DREADDs was evaluated using whole-cell patch clamp electrophysiology on acutely cultured DRG neurons. Pain behavior in mice was assessed using a digging assay, dynamic weight bearing, and rotarod performance, before and after intraperitoneal administration of the DREADD activator, Compound 21.

Results. We showed that AAV-PHP.S can deliver functional genes into ~7% of lumbar DRG neurons when injected into the knee joint in a similar manner to the well-established retrograde tracer, fast blue. Short-term activation of AAV-PHP.S–delivered G_q-DREADD increased excitability of knee neurons in vitro (P = 0.02 by unpaired t-test), without inducing overt pain in mice when activated in vivo. By contrast, in vivo G_i-DREADD activation alleviated digging deficits induced by Freund's complete adjuvant–mediated knee inflammation (P = 0.0002 by repeated-measures analysis of variance [ANOVA] followed by Holm-Sidak multiple comparisons test). A concomitant decrease in knee neuron excitability was observed in vitro (P = 0.005 by ANOVA followed by Holm-Sidak multiple comparisons test).

Conclusion. We describe an AAV-mediated chemogenetic approach to specifically control joint pain, which may be utilized in translational arthritic pain research.

INTRODUCTION

Peripheral sensitization, manifested by an increase in the excitability of dorsal root ganglion (DRG) neurons, underlies many chronic pain pathologies such as inflammatory arthritis (1). DRG neurons display great heterogeneity, based upon both gene expression (2,3) and functional attributes (4), and this heterogeneity is further compounded by target innervation (5,6). The variation in DRG neurons offers a unique opportunity to selectively tune the excitability of a distinct subset of DRG neurons in order to provide

Supported by Versus Arthritis Project (grants RG 20930 and RG 21973 to Dr. Smith). Drs. Chakrabarti and Callejo's work was supported by the Gates Cambridge Trust, the Cambridge Philosophical Society research fund, and University of Cambridge Department of Pharmacology and Corpus Christi College travel awards. Mr. Pattison's work was supported by the University of Cambridge BBSRC Doctoral Training Program (BB/M011194/1).

[1]Sampurna Chakrabarti, BSc, PhD, Luke A. Pattison, BSc, Rebecca H. Rickman, BSc, MPhil, Helen Blake, BA, Gerard Callejo, BSc, PhD, Ewan St. John Smith, MPharmacol, PhD: University of Cambridge, Cambridge, UK; [2]Balint Doleschall, BSc, Paul A. Heppenstall, BSc, PhD (current address Scuola Internazionale Superiore di Studi Avanzati, Trieste, Italy): European Molecular Biology Laboratory, Rome, Italy.

No potential conflicts of interest relevant to this article were reported.

Address correspondence to Ewan St. John Smith, MPharmacol, PhD, University of Cambridge, Department of Pharmacology, Tennis Court Road, Cambridge CB2 1PD, UK. Email: es336@cam.ac.uk.

Submitted for publication February 21, 2020; accepted in revised form May 12, 2020.

pain relief with reduced side effects. For example, we have recently shown that the excitability of knee-innervating DRG neurons (identified by retrograde tracing) is increased in a mouse model of inflammatory joint pain (7) and after incubation with human osteoarthritis (OA) synovial fluid samples (8). These findings suggest that modulation of the knee-innervating DRG neuron subset (knee neurons) could help control arthritic pain.

One way of modulating neuronal excitability is to induce expression of inhibitory or excitatory designer receptors exclusively activated by exogenous chemical actuators, which by themselves do not have any endogenous effects. Modified muscarinic receptor–based designer receptors exclusively activated by designer drugs (DREADDs) is a technology based on this concept, which can increase or decrease neuronal (mostly in the central nervous system [CNS]) firing and which consequently affects a variety of behaviors (9,10), such as enhanced feeding (11) or decreased wakefulness (12). In the peripheral nervous system (PNS), activation of the inhibitory DREADD hM4D(G_i) in voltage-gated sodium channel 1.8 ($Na_V1.8$)–expressing DRG neurons decreased knee hyperalgesia and mechanical allodynia, along with a decrease in DRG neuron firing, in mice with early experimental OA pain induced by surgical destabilization of the medial meniscus (13). This attenuation of hyperalgesia occurred at a similar level compared to the administration of 10 mg/kg morphine, suggesting that peripherally acting analgesics can be comparably potent to well-established opioids.

Similarly, activating G_i-DREADD in transient receptor potential vanilloid 1 (TRPV1)–expressing DRG neurons (14) increased the heat pain threshold and reduced neuronal excitability in mice. Both of those studies used transgenic mice and therefore are less translatable across species due to the technical difficulties associated with targeting sensory neuron subpopulations in species without such transgenic tractability. In wild-type mice, G_i-DREADD delivered intraneurally to the sciatic nerve via adeno-associated virus 6 (AAV6) was able to increase both mechanical and thermal thresholds (15). Importantly, however, none of these studies were specific to DRG neuron subsets innervating specific organs.

AAVs are useful tools for gene transfer that have been used for gene therapy in a variety of human diseases (16), with multiple AAV-based clinical trials currently underway for arthritis (Clinical Trials.gov identifiers: NCT02727764 and NCT02790723) (17). AAVs can be used in conjunction with DREADD technology to selectively modulate neuronal activity of specific neuronal circuitry. Indeed, this has been achieved in the CNS (18). However, delivering genes by AAV injection into a peripheral organ to DRG neurons is challenging because of the low transduction capability of AAVs and the large anatomic distances involved in the PNS (19). A variety of AAV serotypes have shown little efficacy in transducing DRG neurons when injected subcutaneously, intramuscularly, or in an intraplantar manner in adult mice (20,21). To date, direct injection into DRG (22) or intrathecal injection (23,24) are the best ways of transducing DRG neurons. However, these routes of administration are invasive, technically complicated to perform, and do not enable transduction of neurons innervating a defined target. In the present study, we provide evidence that the PNS-specific AAV serotype, AAV-PHP.S (19), can infect DRG neurons with functional cargo following injection into the knee joint. Furthermore, using the inhibitory DREADD, hM4D(G_i), as a cargo, we show that its activation normalizes the inflammatory pain–induced deficit in digging behavior in mice, which is an ethologically relevant spontaneous pain measure indicating well-being (25). Our study thus extends the use of AAV and DREADD technologies to study DRG neurons infected from a peripheral organ, which may have clinically relevant applications in the future in controlling pain pathologies.

MATERIALS AND METHODS

Animals. C57BL/6J (Envigo) mice ages 10–15 weeks (n = 30) of both sexes were used in this study. Mice were housed in groups of up to 5 in a temperature-controlled (21°C) room on a 12-hour light/dark cycle with food, water, and appropriate enrichment available ad libitum. Mice used in this study were regulated under the Animals (Scientific Procedure) Act 1986, Amendment Regulations 2012. All protocols were approved by a UK Home Office project license (P7EBFC1B1) and reviewed by the University of Cambridge Animal Welfare and Ethical Review Body.

Viruses. AAV-PHP.S-CAG-tdTomato (no. 59462-PHP.S) was purchased from Addgene. AAV plasmids for DREADD viruses were also purchased from Addgene (Supplementary Table 1, on the *Arthritis & Rheumatology* website at http://onlinelibrary.wiley.com/doi/10.1002/art.41314/abstract) and packaged at the European Molecular Biology Laboratory in Rome, as previously described (26). Ten 150-mm dishes of HEK293T cells (ATCC) were triple-transfected with plasmids of AAV-PHP.S, helper (Agilent), and cargo in a 1:4:1 ratio with polyethyleneimine (PEI) reagent (1:3 plasmid to PEI ratio; Sigma) (Supplementary Table 1). Three days after transfection, cells and media were collected, and this mixture was centrifuged at 3,700*g* at 4°C to remove debris and then concentrated by ultrafiltration using Vivaflow 200 (Sartorius). The purified AAV particles were collected after running the viral concentrate through an iodixanol column (Opti-Prep density gradient medium; Alere Technologies) by ultracentrifugation (L8-70M; Beckman) at 44,400*g* for 2 hours at 18°C, followed by filtration using a 100-kd filter to further concentrate the sample and for buffer exchange. Viral titers (vg/ml) were measured by probing for woodchuck hepatitis virus posttranscriptional regulatory element regions (forward GGCTGTTGGGCACTGACAAT, reverse CCGAAGGGACGTAGCAGAAG) with quantitative polymerase chain reaction (qPCR) of linearized virus particles with SYBR Green as previously described (26), using a StepOnePlus

Real-Time PCR system according to the guidelines of the manufacturer (Applied Biosystems).

Knee injections. All knee injections were conducted under anesthesia (100 mg/kg ketamine and 10 mg/kg xylazine, intraperitoneally) through the patellar tendon. For experiments with retrograde tracing, 1.5 μl of fast blue or titer-matched AAV-PHP.S viruses were injected intraarticularly into mouse knee joints (~4×10^{11} vg of AAV-PHP.S-CAG-dTomato and ~5×10^{11} vg of AAV-PHP.S packaged with G_i- and G_q-DREADD into each knee). The titer values were chosen based on a pilot experiment conducted with AAV-PHP.S-CAG-YFP, in which injection of 2 μl (~3×10^{11} vg) and 10 μl (~10^{12} vg) labeled a similar number of neurons as assessed by acute culture. For experiments involving inflammation, 7.5 μl Freund's complete adjuvant (CFA) (10 mg/ml; Chondrex) was injected into the left knee, and Vernier calipers were used to measure knee width before and 24 hours after CFA injection (7).

Behavioral testing. All behavioral experiments were carried out between 10:00 AM and 1:00 PM in the presence of 2 investigators (SC and LAP). Mice were assigned randomly to control and experimental groups, and ≥2 cohorts of mice (8–12 mice per group) were assessed in each group on separate days. Mice were trained on digging and rotarod 1 day before the test day. The groups tested in this study are described below.

Compound 21 (C21) controls. As controls, one group of mice did not undergo knee injections. Behavioral tests (described below) were performed on these mice 20 minutes before and after intraperitoneal C21 injection (2 mg/kg diluted in sterile saline from a stock of 100 m*M* in ethanol; Tocris).

Activation of G_q-DREADD. To assess the effects of activation of Gq-DREADD, mice received an intraarticular injection of virus, and 3–4 weeks later were behaviorally tested 20 minutes before and after vehicle injections (1:100 ethanol in sterile saline) or C21 injections.

Activation of G_i-DREADD. To assess the effects of activation of Gi-DREADD, mice received an intraarticular injection of the virus, and 3–4 weeks later, baseline behavioral tests were conducted on mice (pre-CFA). CFA was injected into the knee joints the next day to induce inflammation. Twenty-four hours later, animals were retested 20 minutes before vehicle injections and after vehicle or C21 injections.

Digging. Digging behavior was measured as an assessment of spontaneous pain, as previously described (7), for 3 minutes in a standard cage with a wire lid and filled with Aspen midi 8/20 wood chip bedding (LBS Biotechnology). For training, mice were habituated in the test room in their home cages for 30 minutes, and then they were allowed to dig twice for 3 minutes with a 30-minute break in between. On each subsequent test day, mice were habituated and tested once on the 3-minute paradigm. Test sessions were video-recorded, and the digging duration was later independently coded by investigators who were blinded with regard to the conditions. The number of dig sites (burrows) was coded on test days by the investigators.

Rotarod. Locomotor function and coordination of mice were tested using a rotarod apparatus (Ugo Basile 7650). Mice were tested on a constant-speed rotarod at 7 revolutions per minute for 1 minute, then in an accelerating program (7–40 rpm in 5 minutes) for 6 minutes. The same protocol was used to train mice 1 day before testing. Mice were removed from the rotarod after 2 passive rotations or when they fell from the rotarod. Mice were video-recorded on test days, and 1 investigator who was blinded with regard to the conditions coded these videos for latency(s) to passive rotation or fall.

Dynamic weight bearing. Deficit in weight-bearing capacity is a characteristic measure of spontaneous inflammatory pain behavior, and we measured this behavior using a dynamic weight bearing device (Bioseb) in freely moving mice for 3 minutes. Animals were not trained on this device, and coding was done by 1 investigator who was blinded with regard to the conditions. In ≥1 minute and 30 seconds of the 3-minute recording, fore paw and hind paw prints were identified using the 2 highest confidence levels (based on correlation between manual software algorithm tracking) of the built-in software, ≥30 seconds of which was manually verified.

DRG neuron culture. Lumbar DRG (L2–L5) were collected from a subset of mice in the vehicle group 3-4 weeks after virus injections in ice-cold dissociation media (7). DRG were then enzymatically digested followed by mechanical trituration (7). Dissociated DRG neurons, thus isolated, were then plated onto poly-D-lysine– and laminin-coated glass-bottomed dishes (P35GC-1.5-14-C; MatTek) in DRG culture medium (L-15 Medium [1×] + GlutaMAX-I, 10% [volume/volume] fetal bovine serum, 24 m*M* $NaHCO_3$, 38 m*M* glucose, 2% penicillin/streptomycin) and maintained overnight (8–10 hours) in a humidified incubator at 37°C with 5% CO_2.

Electrophysiology. For control experiments, DRG neurons were bathed in extracellular solution (ECS) containing 140 m*M* NaCl, 4 m*M* KCl, 1 m*M* $MgCl_2$, 2 m*M* $CaCl_2$, 4 m*M* glucose, and 19 m*M* HEPES, adjusted to pH 7.4 with NaOH while recording. To investigate effects of C21 activation, neurons were incubated 10 minutes prior to the start of recording and throughout the recordings in 10 n*M* C21 (diluted in ECS from 100 m*M* stock). Only virus-transduced mice that were identified by their fluorescence upon excitation with a 572-nm LED (Cairn Research) were recorded, using patch pipettes of 5–10 MΩ (P-97 Flaming/Brown puller; Sutter Instruments) with intracellular solution containing 110 m*M* KCl, 10 m*M* NaCl, 1 m*M* $MgCl_2$, 1 m*M* EGTA, 10 m*M*

HEPES, 2 m*M* Na_2ATP, and 0.5 m*M* Na_2GTP, adjusted to pH 7.3 with KOH.

Action potentials (APs) were recorded in current clamp mode without current injection (to investigate spontaneous AP firing) or after stepwise injection of 80 msec current pulses from 0 to 1,050 pA in 50 pA steps using a HEKA EPC-10 amplifier (Lambrecht) and corresponding Patchmaster software. AP properties were analyzed using Fitmaster software (HEKA) or IgorPro software (Wavemetrics) as previously described (7). Neurons were excluded from analysis if they did not fire an AP in response to current injections.

Immunohistochemistry. Mice with unilateral co-injections of AAV-PHP.S-tdTomato (2 μl) and fast blue (1.5 μl) were transcardially perfused with 4% (weight/volume [w/v]) paraformaldehyde (in phosphate buffered saline [PBS], pH 7.4) under terminal anesthesia (sodium pentobarbital, 200 mg/kg, intraperitoneal). L2–L5 DRG were then collected from the injected side, while L3–L4 DRG were collected from the uninjected side and postfixed in Zamboni's fixative for 1 hour, followed by overnight incubation in 30% (w/v) sucrose (in PBS) at 4°C for cryoprotection. DRG were then embedded, snap-frozen, sectioned, and stained as previously described (7), using anti-TRPV1 antibody (1:500; AGP-118, anti–guinea pig polyclonal; Alomone) with Alexa Fluor 488–conjugated secondary antibody (1:500; 706-545-148, anti–guinea pig polyclonal; The Jackson Laboratory). Positive neurons were scored as previously described (7), using an R toolkit (https://github.com/amapruns/Immunohistochemistry_Analysis) followed by manual validation. Briefly, mean gray value (intensity) of all neurons in 1–3 sections from each DRG level of interest in each mouse was measured using ImageJ. A neuron was scored as positive for a stain if it had an intensity value >2 SDs above the average normalized minimum gray value across all sections.

Statistical analysis. Comparisons between 2 groups were made using the appropriate Student's *t*-test (paired for repeated measures and unpaired otherwise), while 3-group comparisons were made using repeated-measures or one-way analysis of variance (ANOVA) followed by Holm-Sidak multiple comparisons tests. Chi-square tests were used to compare proportions of categorical variables. Data are presented as the mean ± SEM.

RESULTS

Robust transduction of DRG neurons by knee-injected AAV-PHP.S. AAV-PHP.S was engineered to have a higher specificity toward peripheral neurons (19), and thus we hypothesized that this AAV serotype would be able to transduce DRG neurons when injected intraarticularly into the knee joint. Consistent with our hypothesis, when AAV-PHP.S-CAG-dTomato and the commonly used retrograde tracer, fast blue, were co-injected unilaterally into 1 knee in mice (n = 3, all female), we observed both fast blue and virus labeling (Figure 1A). Comparable to findings of previous studies that used fast blue and other retrograde tracers (7,27,28), we observed a similar proportion of labeling in the lumbar DRG neurons with fast blue and AAV-PHP.S-CAG-dTomato (Figure 1B). Across L2–L5 DRG, there was ~40% co-labeling of neurons with fast blue and AAV-PHP.S-CAG-dTomato, which suggests that neither retrograde tracer is able to label the entire knee neuron population (Figure 1C and Supplementary Figure 1,

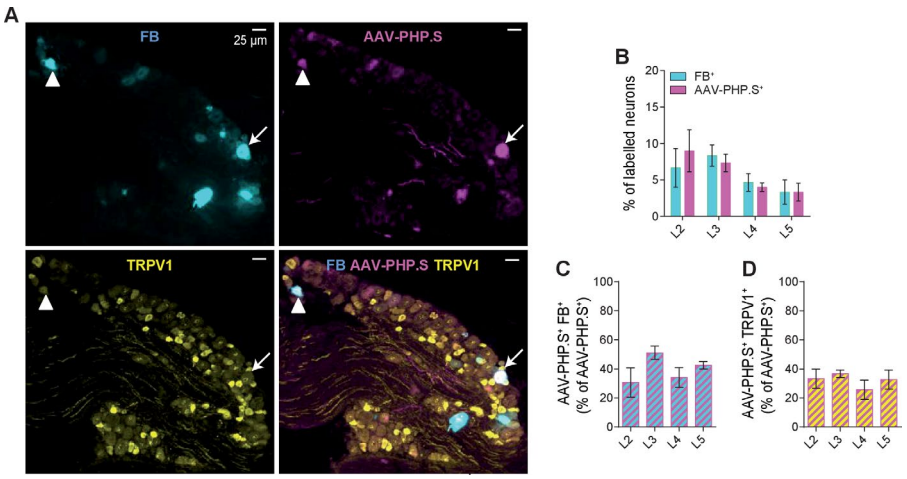

Figure 1. Retrograde tracing of knee-innervating dorsal root ganglion (DRG) neurons using fast blue (FB) and an adeno-associated virus (AAV) product, AAV-PHP.S-CAG-dTomato. **A**, Representative images of a whole L3 DRG section showing knee neurons traced using fast blue (blue) or AAV-PHP.S-CAG-dTomato (pink), and stained using an anti–transient receptor potential vanilloid channel 1 (TRPV1) antibody (yellow). **Arrowheads** point to a neuron with fast blue, AAV-PHP.S, and TRPV1 colocalization; **arrows** point to a neuron that shows only fast blue and AAV-PHP.S colocalization. **B**, Percentage of neurons in L2–L5 DRG labeled with fast blue and AAV-PHP.S. **C** and **D**, Percentage of neurons showing colocalization of fast blue and AAV-PHP.S (**C**) and TRPV1 and AAV-PHP.S (**D**), expressed as a percentage of AAV-PHP.S–positive neurons. Bars show the mean ± SEM from 3 female mice.

http://onlinelibrary.wiley.com/doi/10.1002/art.41314/abstract). However, area analysis of the labeled neurons suggests that similar-sized neurons are targeted by both strategies (Supplementary Figure 1). Furthermore, we observed minimum labeling in the contralateral side (Supplementary Figure 1).

Previous studies suggest that ~40% of knee neurons are TRPV1-expressing putative nociceptors (7,28). Similarly, through immunohistochemical analysis of DRG neurons, we found that ~30% of virus-labeled and fast blue–labeled neurons (mostly small-diameter neurons) express TRPV1 (Figure 1D and Supplementary Figure 1, http://onlinelibrary.wiley.com/doi/10.1002/art.41314/abstract), suggesting that viral transduction did not substantially alter expression of the nociceptive protein, TRPV1. Taken together, these findings indicate that intraarticular injection of AAV-PHP.S--CAG-dTomato in the knee joint transduces mouse DRG neurons in a similar manner to that of a routinely used retrograde tracer.

Spontaneous pain behavior is unchanged by excitatory G_q-DREADD delivered intraarticularly by AAV-PHP.S-hSyn-hM3D(G_q)-mCherry, but motor coordination deficit is provoked. Next, we tested whether AAV-PHP.S can deliver functional hM3D(G_q) cargo into knee neurons via intraarticular

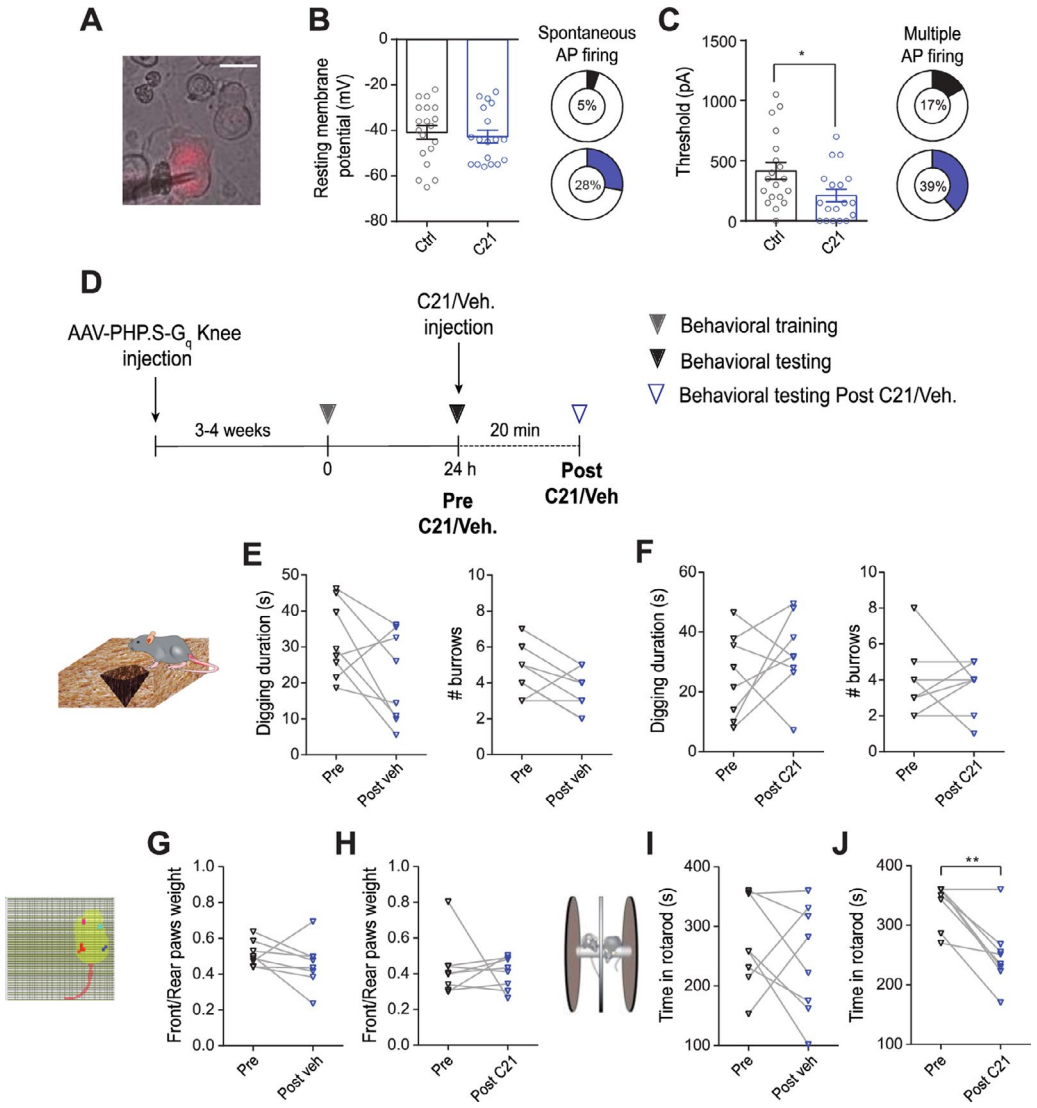

Figure 2. G_q–designer receptor exclusively activated by designer drugs (DREADD) activation of mouse knee neurons in vitro and in vivo. **A**, Representative image of neuron transduced by adeno-associated virus product AAV-PHP.S-hSyn-hM$_3$D(G_q)-mCherry (bar = 25 μm; triangular shadow = recording electrode). **B** and **C**, Resting membrane potential and spontaneous action potential (AP) firing (**B**) and threshold and multiple AP firing (**C**) under control (ctrl) conditions (n = 19 neurons) and with Compound 21 (C21) treatment (n = 18 neurons). Data were obtained using 2 male and 3 female mice. Each symbol represents an individual neuron; bars show the mean ± SEM. **D**, Timeline showing when behaviors were assessed. **E**–**J**, Digging duration and number of burrows, ratio of front and rear paw weight, and rotarod behavior before and after vehicle (veh) injection (**E**, **G**, and **I**) or before and after C21 injection (**F**, **H**, and **J**). Each symbol represents an individual mouse (n = 4 male and 4 female mice); bars show the mean ± SEM. * = $P < 0.05$ by unpaired *t*-test; ** = $P < 0.01$ by paired *t*-test. Color figure can be viewed in the online issue, which is available at http://onlinelibrary.wiley.com/doi/10.1002/art.41314/abstract.

injection, using whole-cell patch clamp on acutely dissociated neurons isolated from mice with no previous exposure to the DREADD activator C21. C21 was chosen as the DREADD activator since it has good bioavailability (57% plasma concentration 1 hour postinjection), is not converted into clozapine or clozapine *N*-oxide (29), and had no off-target effect in the behavioral tests conducted in naive mice not injected with DREADDs (Supplementary Figure 2, http://onlinelibrary.wiley.com/doi/10.1002/art.41314/abstract). G_q-DREADDs couple to G_qPCR pathways, and their activation causes neuronal excitation (9). Therefore, we hypothesized that when incubated with 10 n*M* C21, virally transduced neurons would be hyperexcitable compared to virally transduced neurons bathed in normal ECS. In accordance with this hypothesis, we observed an increased number of small- and medium-diameter (Supplementary Figure 3, http://onlinelibrary.wiley.com/doi/10.1002/art.41314/abstract), mostly nociceptive neurons (characterized by an AP half-peak duration of >1 msec and a "hump" during repolarization) firing APs without injection of current in the C21 group (vehicle group 5.3% versus C21 group 27.8%; $P = 0.03$ by chi-square test) (30) (Figures 2A and B and Supplementary Figure 3, http://onlinelibrary.wiley.com/doi/10.1002/art.41314/abstract).

Moreover, upon increased stepwise current injections, the AP threshold was decreased in the C21 group ($P = 0.02$ by unpaired *t*-test) (Figure 2C); no change was observed in other electrical properties measured in these neurons (Table 1). Our data also suggest that virally transduced neurons are viable, because the reported AP threshold is very similar to what we have previously observed in fast blue–positive knee-innervating neurons (31).

Based on previous studies (7,8), we hypothesized that the increased excitability of knee-innervating neurons in vitro via the G_q-DREADD system would cause pain-like behavior in mice in vivo, which was tested by assessing digging behavior (a measure of spontaneous pain as previously described [7,32]), dynamic weight bearing, and rotarod behavior (a measure of motor coordination [33]) (Figure 2D). Three weeks after virus injection into both knee joints, mice injected with vehicle or C21 (n = 4 male and 4 female mice in each group) did not show significant changes in digging behavior (mean ± SEM digging duration pre-vehicle 31.6 ± 3.7 seconds versus post-vehicle 21.3 ± 4.4 seconds; mean ± SEM digging duration pre-C21 25.2 ± 4.9 seconds versus post-C21 32.7 ± 4.7 seconds; mean ± SEM number of burrows pre-vehicle 4.6 ± 0.5 versus post-vehicle 3.5 ± 0.4; mean ± SEM number of burrows pre-C21 3.9 ± 0.7 versus post-C21 3.6 ± 0.5) (Figures 2E and F) or weight bearing (mean ± SEM front paw to rear paw weight ratio pre-vehicle 0.5 ± 0.02 versus post-vehicle 0.5 ± 0.04; mean ± SEM front paw to rear paw weight ratio pre-C21 0.4 ± 0.06 versus post-C21 0.4 ± 0.03) (Figures 2G and H).

Table 1. AP properties of mouse knee neurons intraarticularly transduced with G_q-DREADD*

	Control group (n = 19)	C21 group (n = 18)
RMP, mV	−40.8 ± 3.0	−42.7 ± 2.8
Threshold, pA	415.8 ± 69.7	211.1 ± 51.4†
HPD, msec	2.6 ± 0.5	1.9 ± 0.3
AHP peak, mV	14.7 ± 2.1	16.8 ± 2.8

* Values are the mean ± SEM. AP = action potential; DREADD = designer receptor exclusively activated by designer drugs; C21 = Compound 21; RMP = resting membrane potential; HPD = half-peak duration; AHP = afterhyperpolarization.
† $P < 0.05$ versus control group, by unpaired *t*-test.

By contrast, after injection of C21, mice showed a marked decline in their ability to remain on the rotarod (mean ± SEM pre-vehicle 273.5 ± 27.2 seconds versus post-vehicle 243.9 ± 32.7 seconds; mean ± SEM pre-C21 336.1 ± 12.9 seconds versus post-C21 249.0 ± 18.9 seconds; $P = 0.002$ by paired *t*-test), suggesting a deficit in their motor coordination (Figures 2I and J). DRG for all virus-injected mice were evaluated under a fluorescence microscope to check for viral transduction, and a subset of these DRG were further analyzed to reveal similar transduction profiles between AAV-PHP.S-hSyn-G_q-DREADD-mCherry and AAV-PHP.S-CAG-dTomato (i.e., different promoters do not significantly affect transduction) (Supplementary Figure 3, http://onlinelibrary.wiley.com/doi/10.1002/art.41314/abstract). Taken together, our findings show that AAV-PHP.S delivers functional G_q-DREADD into knee neurons and that when virally transduced knee neurons are activated, they do not produce overt pain-like behavior in vivo but do cause a deficit in motor coordination.

Digging behavior deficits associated with inflammatory pain are reversed by inhibitory G_i-DREADD delivered intraarticularly by AAV-PHP.S-hSyn-hM4D(G_i)-mCherry. Intraarticular injection of CFA induced robust knee inflammation in mice (mean ± SEM control knee width pre-CFA 3.1 ± 0.03 mm versus post-CFA 3.1 ± 0.03 mm; mean ± SEM CFA knee width pre-CFA 3.1 ± 0.02 mm versus post-CFA 4.0 ± 0.05 mm; n = 24; $P < 0.0001$ by paired *t*-test) (Figure 3A) and was previously shown to increase the excitability of knee neurons innervating the inflamed knee compared to those innervating the contralateral side (7). The post-CFA knee measurements were conducted at the end of behavioral measurements, suggesting that regardless of G_i-DREADD activation, knee inflammation persisted at 24 hours post–CFA injection.

We hypothesized that incubating G_i-DREADD–expressing knee neurons from the CFA side with C21 would reverse this increased neuronal excitability. Using whole-cell patch clamp electrophysiology of small- and medium-diameter knee neurons (Supplementary Figure 4, http://onlinelibrary.wiley.com/doi/10.1002/art.41314/abstract), the percentage of CFA knee neurons firing spontaneous APs was found to be decreased after G_i-DREADD activation (CFA 15% versus CFA + C21 0%; $P = 0.02$ by chi-square test) (Figure 3C and Supplementary Figure 3, http://onlinelibrary.wiley.com/doi/10.1002/art.41314/abstract), although there

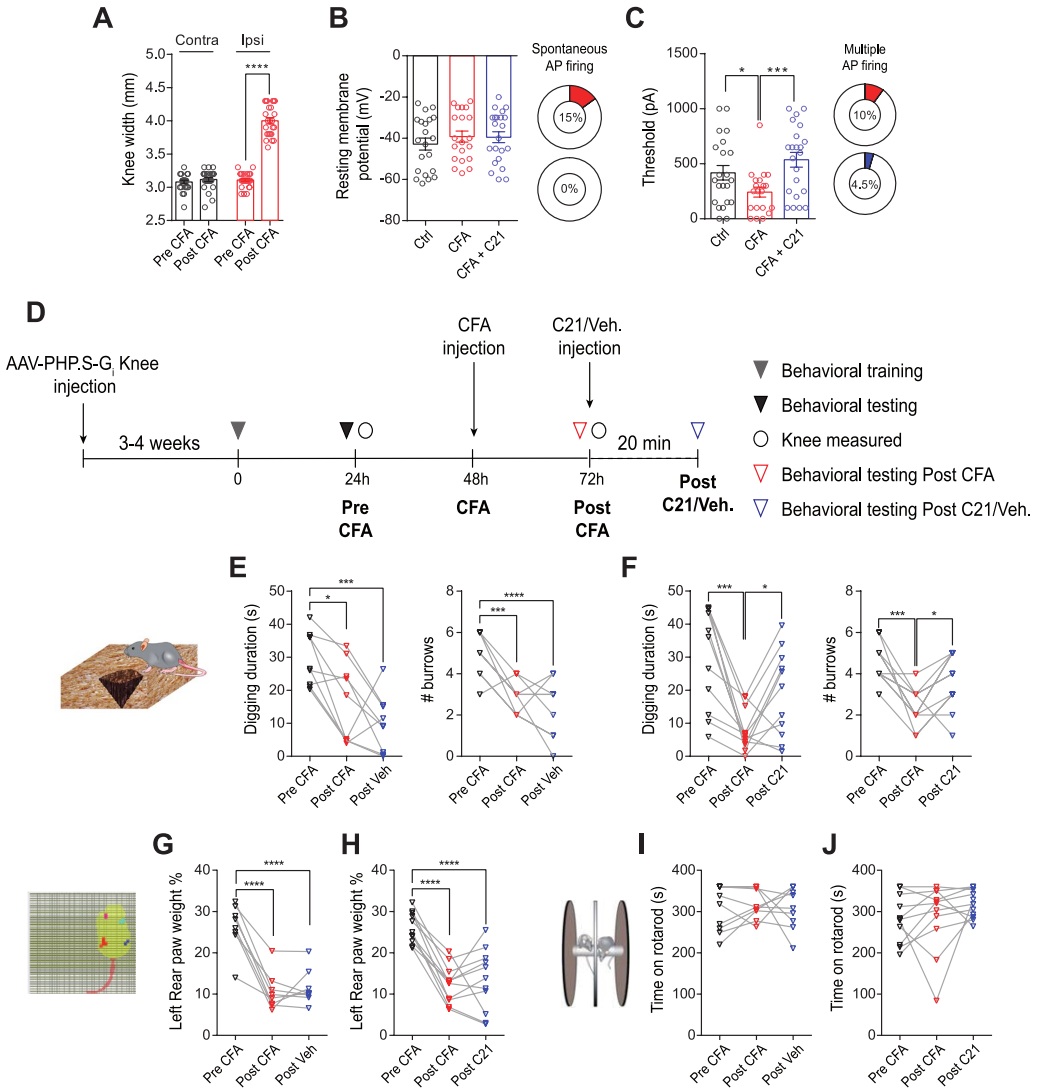

Figure 3. G_i-DREADD activation of mouse knee neurons in vitro and in vivo. **A**, Knee width before and after Freund's complete adjuvant (CFA) injection in the uninjected contralateral knee (contra) and injected ipsilateral knee (ipsi) (n = 20). **B** and **C**, Resting membrane potential and spontaneous AP firing (**B**) and threshold and multiple AP firing (**C**) under control conditions (n = 22 neurons), with CFA treatment (n = 20 neurons), and with CFA and C21 treatment (n = 22 neurons). Data were obtained using 2 male and 2 female mice. **D**, Timeline showing when behaviors were assessed. **E**–**J**, Digging duration and number of burrows, rear left paw weight expressed as percentage of body weight, and rotarod behavior before and after CFA treatment and after vehicle treatment (**E**, **G**, and **I**) (n = 5 male and 4 female mice) or before and after CFA treatment and after C21 injection (**F**, **H**, and **J**) (n = 7 male and 4 female mice). Each symbol represents an individual mouse; bars show the mean ± SEM. In **A**, **** = $P < 0.0001$ by paired *t*-test. In all other graphs, * = $P < 0.05$; *** = $P < 0.001$; **** = $P < 0.0001$, by repeated-measures analysis of variance followed by Holm-Sidak multiple comparisons test. See Figure 2 for other definitions. Color figure can be viewed in the online issue, which is available at http://onlinelibrary.wiley.com/doi/10.1002/art.41314/abstract.

was no change in the resting membrane potential across all conditions (Figure 3B and Table 2). Moreover, in the absence of G_i-DREADD activation, CFA knee neurons had a decreased AP threshold compared to neurons from the control side, but the AP threshold of CFA knee neurons that were incubated with C21 was similar to that of neurons from the control side ($P = 0.005$ by ANOVA followed by Holm-Sidak multiple comparisons test; Figure 3C). These results suggest that G_i-DREADD activation reverses a CFA-induced increase in nociceptor excitability in vitro (Supplementary Figure 4). Other electrical properties between groups were unchanged (Table 2).

The ability of G_i-DREADD to modulate pain behavior in DRG neurons is unclear, with one study showing an increase in latency to both thermal and mechanical stimuli (15) but another showing only an increase in the paw withdrawal latency to thermal stimuli (14). Nevertheless, based on the in vitro results in these studies, we hypothesized that activation of G_i-DREADDs in knee neurons post–CFA injection would reverse spontaneous pain behavior

Table 2. AP properties of mouse knee neurons intraarticularly transduced with G_i-DREADD*

	Control group (n = 22)	CFA group (n = 20)	CFA + C21 group (n = 22)
RMP, mV	−42.9 ± 2.9	−39.2 ± 2.7	−39.5 ± 2.7
Threshold, pA	418.2 ± 65.6†	242.5 ± 45.0	536.4 ± 66.5‡
HPD, msec	2.4 ± 0.6	2.9 ± 0.5	2.1 ± 0.3
AHP peak, mV	12.9 ± 1.3	16.5 ± 1.3	13.8 ± 1.6

* Values are the mean ± SEM. CFA = Freund's complete adjuvant (see Table 1 for other definitions).
† $P < 0.05$ versus CFA group, by analysis of variance (ANOVA) followed by Holm-Sidak multiple comparisons test.
‡ $P < 0.01$ versus CFA group, by ANOVA followed by Holm-Sidak multiple comparisons test.

in mice (Figure 3D). In the control cohort that received vehicle 24 hours after CFA injection (n = 5 male and 4 female mice), the CFA-induced decrease in digging behavior persisted compared to pre-CFA (mean ± SEM digging duration pre-CFA 29.6 ± 2.7 seconds, post-CFA 16.6 ± 4.0 seconds, post-vehicle 9.8 ± 2.8 seconds; $P = 0.0005$, pre-CFA versus post-vehicle) (mean ± SEM number of burrows pre-CFA 4.8 ± 0.3, post-CFA 2.9 ± 0.3, post-vehicle 2.3 ± 0.5; n = 9; $P < 0.0001$ by repeated-measures ANOVA [RM-ANOVA] followed by Holm-Sidak multiple comparisons test) (Figure 3E).

However, when C21 was administered to a separate cohort of mice 24 hours after CFA injection (n = 7 male and 4 female mice), there was a marked recovery in digging behavior (mean ± SEM digging duration pre-CFA 29.7 ± 4.5 seconds, post-CFA 7.8 ± 1.9 seconds, post-C21 19.0 ± 3.9 seconds; $P = 0.0002$) (mean ± SEM number of burrows pre-CFA, 4.5 ± 0.3, post-CFA 2.4 ± 0.3, post-C21 3.6 ± 1.4; $P = 0.0005$ by RM-ANOVA followed by Holm-Sidak multiple comparisons test) (Figure 3F). These findings suggest that decreasing the excitability of knee neurons via G_i-DREADD reduces inflammation-induced spontaneous pain that is associated with an increased sense of well-being demonstrated by more digging. In contrast, acute chemogenetic inhibition of knee neurons was insufficient to reverse the CFA-induced deficit in dynamic weight bearing as a percentage of body weight (mean ± SEM rear left weight bearing pre-CFA 26.2 ± 2.0%, post-CFA 10.6 ± 1.7%, post-vehicle 11.6 ± 1.5%; $P < 0.0001$; mean ± SEM rear left weight bearing pre-CFA 26.1 ± 1.1%, post-CFA 12.4 ± 1.4%, post-C21 13.3 ± 2.2%; $P < 0.0001$ by RM-ANOVA followed by Holm-Sidak multiple comparisons test) (Figures 3G and H). This may be because gait changes relating to weight bearing are more reflective of changes in joint biomechanics that are difficult to reverse with analgesics (34).

Furthermore, no change in rotarod behavior was observed following CFA-induced knee inflammation, suggesting that this model does not cause an overt change in gross motor function and similarly that G_i-DREADD activation had no effect (mean ± SEM time on rotarod pre-CFA 303.8 ± 18.3 seconds, post-CFA 315.9 ± 11.9 seconds, post-vehicle 306.6 ± 16.8 seconds; mean ± SEM time on rotarod pre-CFA 282.7 ± 17.3 seconds, post-CFA 286.4 ± 25.3 seconds, post-C21 317.4 ± 10.3 seconds) (Figures 3I and J). DRG for all virus-injected mice were evaluated under a fluorescence microscope to check for viral transduction (Supplementary Figure 4, http://onlinelibrary.wiley.com/doi/10.1002/art.41314/abstract). Taken together, our findings indicate that specific inhibition of knee neuron excitability can reverse inflammation-induced deficits in digging behavior.

DISCUSSION

We found that the AAV-PHP.S serotype can provide retrograde cargo delivery to DRG neurons in a peripheral tissue–specific manner when injected into the mouse knee joints, without the need for invasive procedures or the requirement to generate transgenic mice. The transduction efficacy of the virus is similar to that of the widely used retrograde tracer, fast blue. Consistent with findings of other co-labeling studies (35), the ~40% colocalization of AAV-PHP.S and fast blue fluorescence suggests that not all knee neurons are labeled with either tracer and that co-labeling of <100% is possibly due to their differing modes of retrograde transfer (36,37). Furthermore, we report that ~30% of labeled neurons are TRPV1+, which fits with the previously reported identity of knee-innervating neurons as a subset being ~39% TRPV1+, ~53% CGRP+, and largely isolectin B4–nonbinding (28,38).

Using this model, we have shown that it is possible to increase or decrease knee neuron excitability in vitro when G_q- or G_i-DREADD cargoes were delivered, respectively, by AAV-PHP.S and to provide joint-specific pain control. This result can also be extended to study the role of anatomically specific neuronal excitability when exposed to a variety of stimuli or pharmacologic interventions. In vivo, we restricted our chemogenetic activation to a short duration in order to reflect acute pain, and within this timeframe we observed no spontaneous pain-like behavior with the activation of G_q-DREADD in knee neurons. We surmised that G_q-mediated subthreshold activation (39) of the relatively low percentage of DRG neurons did not provide sufficient nociceptive input to drive change in ethologically relevant pain behavior, whereas the observed decrease in coordination suggests that we behaviorally engaged the virally transduced neurons. Furthermore, we noted that the intraarticular injection described here would transduce DREADDs to both nociceptive and non-nociceptive populations of knee neurons, and therefore, a clear nocifensive behavior might not be apparent. In other words, a limitation of this study is that

distinct subpopulations of knee neurons are not targeted, but future studies could address this once such populations have been described for the knee, as has already been conducted for the colon (5). Future studies using a repeated dosing strategy could also be employed in our system for modeling chronic pain, being cautious of the potential risk of receptor desensitization (9).

Perhaps more relevant to future clinical applications in arthritic pain is the ability of G_i-DREADDs to reverse pain behavior by decreasing neuronal excitability of knee neurons. Indeed, we have shown that G_i-DREADD activation restores a deficit in digging behavior induced by inflammatory knee pain, similar to previous studies demonstrating normalization of burrowing/digging by nonsteroidal antiinflammatory drugs (40,41) and a peripherally restricted TRPV1 antagonist (7) after joint pain–induced depression of this behavior. This strategy can be further refined to selectively inhibit genetically specific subpopulations of knee neurons by combining Cre-inducible viruses with their corresponding Cre-expressing transgenic mouse lines, thereby providing insights into relative contributions of different knee neuron subpopulations in arthritic pain. Selectively exciting specific knee neuron subpopulations with G_q-DREADD might produce pain-like behaviors that were not observed in this study. We also observed that the CFA-induced deficit in weight bearing was not reversed following the activation of G_i-DREADD in knee neurons, consistent with a previous study demonstrating that reversal of deficits in gait changes are difficult to achieve with analgesics (34).

Although the findings of this study imply that modulating excitability of anatomically specific peripheral neurons could control arthritic pain, a number of challenges remain to be addressed before their clinical translation. Since virus transduction and expression profile is different between nonhuman primates and rodents, the expression profile of AAV-PHP.S needs to first be validated in nonhuman primates (42). Additional work is also required to engineer more PNS-specific AAVs and to optimize DREADDs (43) and their corresponding ligands (44) for increasing transduction efficiency and regulating dosing. Overall, the present study provides initial proof of concept that peripheral tissue–innervating DRG neurons can be specifically modulated by AAVs, opening the door to future studies on gene therapy in controlling arthritic pain.

ACKNOWLEDGMENTS

We thank Morris Poeuw and Fernanda Castro de Reis for technical help with viral production, Julie Gautrey and Anne Desevre for technical help with mouse behavior, and Dewi Safitri for graphic design.

AUTHOR CONTRIBUTIONS

All authors were involved in drafting the article or revising it critically for important intellectual content, and all authors approved the final version to be published. Dr. Smith had full access to all of the data in the study and takes responsibility for the integrity of the data and the accuracy of the data analysis.

Study conception and design. Chakrabarti, Pattison, Heppenstall, Smith.

Acquisition of data. Chakrabarti, Pattison, Doleschall, Rickman, Blake, Callejo.

Analysis and interpretation of data. Chakrabarti, Heppenstall, Smith.

REFERENCES

1. Walsh DA, McWilliams DF. Mechanisms, impact and management of pain in rheumatoid arthritis [review]. Nat Rev Rheumatol 2014;10:581–92.
2. Zeisel A, Hochgerner H, Lönnerberg P, Johnsson A, Memic F, van der Zwan J, et al. Molecular architecture of the mouse nervous system. Cell 2018;174:999–1014.e22.
3. North RY, Li Y, Ray P, Rhines LD, Tatsui CE, Rao G, et al. Electrophysiological and transcriptomic correlates of neuropathic pain in human dorsal root ganglion neurons. Brain 2019;142:1215–26.
4. Petruska JC, Napaporn J, Johnson RD, Gu JG, Cooper BY. Subclassified acutely dissociated cells of rat DRG: histochemistry and patterns of capsaicin-, proton-, and ATP-activated currents. J Neurophysiol 2000;84:2365–79.
5. Hockley JR, Taylor TS, Callejo G, Wilbrey AL, Gutteridge A, Bach K, et al. Single-cell RNAseq reveals seven classes of colonic sensory neuron. Gut 2019;68:633–44.
6. Immke DC, McCleskey EW. Lactate enhances the acid-sensing Na^+ channel on ischemia-sensing neurons. Nat Neurosci 2001;4:869–70.
7. Chakrabarti S, Pattison LA, Singhal K, Hockley JR, Callejo G, Smith ES. Acute inflammation sensitizes knee-innervating sensory neurons and decreases mouse digging behavior in a TRPV1-dependent manner. Neuropharmacology 2018;143:49–62.
8. Chakrabarti S, Jadon DR, Bulmer DC, Smith ES. Human osteoarthritic synovial fluid increases excitability of mouse dorsal root ganglion sensory neurons: an in-vitro translational model to study arthritic pain. Rheumatology (Oxford) 2020;59:662–7.
9. Roth BL. DREADDs for neuroscientists. Neuron 2016;89:683–94.
10. Alles SR, Malfait AM, Miller RJ. Chemo- and optogenetic strategies for the elucidation of pain pathways. In: Wood JN, editor. The Oxford handbook of the neurobiology of pain. Oxford University Press; 2019. URL: https://www.oxfordhandbooks.com/view/10.1093/oxfordhb/9780190860509.001.0001/oxfordhb-9780190860509-e-33.
11. Krashes MJ, Koda S, Ye C, Rogan SC, Adams AC, Cusher DS, et al. Rapid, reversible activation of AgRP neurons drives feeding behavior in mice. J Clin Invest 2011;121:1424–8.
12. Sasaki K, Suzuki M, Mieda M, Tsujino N, Roth B, Sakurai T. Pharmacogenetic modulation of orexin neurons alters sleep/wakefulness states in mice. PLoS One 2011;6:e20360.
13. Miller RE, Ishihara S, Bhattacharyya B, Delaney A, Menichella DM, Miller RJ, et al. Chemogenetic inhibition of pain neurons in a mouse model of osteoarthritis. Arthritis Rheumatol 2017;69:1429–39.
14. Saloman JL, Scheff NN, Snyder LM, Ross SE, Davis BM, Gold MS. Gi-DREADD expression in peripheral nerves produces ligand-dependent analgesia, as well as ligand-independent functional changes in sensory neurons. J Neurosci 2016;36:10769–81.
15. Iyer SM, Vesuna S, Ramakrishnan C, Huynh K, Young S, Berndt A, et al. Optogenetic and chemogenetic strategies for sustained inhibition of pain. Sci Rep 2016;6:30570.
16. Wang D, Tai PW, Gao G. Adeno-associated virus vector as a platform for gene therapy delivery [review]. Nat Rev Drug Discov 2019;18:358–78.
17. ClinicalTrials.gov. National Library of Medicine: National Institutes of Health clinical trials database. URL: http://www.clinicaltrials.gov/.

18. Aschauer DF, Kreuz S, Rumpel S. Analysis of transduction efficiency, tropism and axonal transport of AAV serotypes 1, 2, 5, 6, 8 and 9 in the mouse brain. PLoS One 2013;8:e76310.
19. Chan KY, Jang MJ, Yoo BB, Greenbaum A, Ravi N, Wu WL, et al. Engineered AAVs for efficient noninvasive gene delivery to the central and peripheral nervous systems. Nat Neurosci 2017;20:1172–9.
20. Towne C, Pertin M, Beggah AT, Aebischer P, Decosterd I. Recombinant adeno-associated virus serotype 6 (rAAV2/6)-mediated gene transfer to nociceptive neurons through different routes of delivery. Mol Pain 2009;5:52.
21. Abdallah K, Nadeau F, Bergeron F, Blouin S, Blais V, Bradbury KM, et al. Adeno-associated virus 2/9 delivery of Cre recombinase in mouse primary afferents. Sci Rep 2018;8:7321.
22. Mason MR, Ehlert EM, Eggers R, Pool CW, Hermening S, Huseinovic A, et al. Comparison of AAV serotypes for gene delivery to dorsal root ganglion neurons. Mol Ther 2010;18:715–24.
23. Storek B, Harder NM, Banck MS, Wang C, McCarty DM, Janssen WG, et al. Intrathecal long-term gene expression by self-complementary adeno-associated virus type 1 suitable for chronic pain studies in rats. Mol Pain 2006;2:4.
24. Weir GA, Middleton SJ, Clark AJ, Daniel T, Khovanov N, McMahon SB, et al. Using an engineered glutamate-gated chloride channel to silence sensory neurons and treat neuropathic pain at the source. Brain 2017;140:2570–85.
25. Jirkof P. Burrowing and nest building behavior as indicators of well-being in mice. J Neurosci Methods 2014;234:139–46.
26. Challis RC, Kumar SR, Chan KY, Challis C, Beadle K, Jang MJ, et al. Systemic AAV vectors for widespread and targeted gene delivery in rodents. Nat Protoc 2019;14:379–414.
27. Ferreira-Gomes J, Adães S, Sarkander J, Castro-Lopes JM. Phenotypic alterations of neurons that innervate osteoarthritic joints in rats. Arthritis Rheum 2010;62:3677–85.
28. Cho WG, Valtschanoff JG. Vanilloid receptor TRPV1-positive sensory afferents in the mouse ankle and knee joints. Brain Res 2008;1219:59–65.
29. Jendryka M, Palchaudhuri M, Ursu D, van der Veen B, Liss B, Kätzel D, et al. Pharmacokinetic and pharmacodynamic actions of clozapine-N-oxide, clozapine, and compound 21 in DREADD-based chemogenetics in mice. Sci Rep 2019;9:4522.
30. Djouhri L, Lawson SN. Changes in somatic action potential shape in guinea-pig nociceptive primary afferent neurones during inflammation in vivo. J Physiol 1999;520:565–76.
31. Chakrabarti S, Hore Z, Pattison LA, Lalnunhlimi S, Bhebhe CN, Callejo G, et al. Sensitization of knee-innervating sensory neurons by tumor necrosis factor-α activated fibroblast-like synoviocytes: an in vitro, co-culture model of inflammatory pain. Pain 2020. E-pub ahead of print.
32. Deacon RM. Digging and marble burying in mice: simple methods for in vivo identification of biological impacts. Nat Protoc 2006;1:122–4.
33. Tappe-Theodor A, King T, Morgan MM. Pros and cons of clinically relevant methods to assess pain in rodents [review]. Neurosci Biobehav Rev 2019;100:335–43.
34. Shepherd AJ, Mohapatra DP. Pharmacological validation of voluntary gait and mechanical sensitivity assays associated with inflammatory and neuropathic pain in mice. Neuropharmacology 2018;130:18–29.
35. Puigdellívol-Sánchez A, Prats-Galino A, Ruano-Gil D, Molander C. Efficacy of the fluorescent dyes fast blue, fluoro-gold, and diamidino yellow for retrograde tracing to dorsal root ganglia after subcutaneous injection. J Neurosci Methods 1998;86:7–16.
36. Eisenman LM. Uptake of the retrograde fluorescent tracer fast blue from the cerebrospinal fluid of the rat. Neurosci Lett 1985;60:241–6.
37. Tervo DG, Hwang BY, Viswanathan S, Gaj T, Lavzin M, Ritola KD, et al. A designer AAV variant permits efficient retrograde access to projection neurons. Neuron 2016;92:372–82.
38. Ivanavicius S, Blake D, Chessell I, Mapp P. Isolectin B4 binding neurons are not present in the rat knee joint. Neuroscience 2004;128:555–60.
39. Jaiswal PB, English AW. Chemogenetic enhancement of functional recovery after a sciatic nerve injury. Eur J Neurosci 2017;45:1252–7.
40. Gould SA, Doods H, Lamla T, Pekcec A. Pharmacological characterization of intraplantar Complete Freund's Adjuvant-induced burrowing deficits. Behav Brain Res 2016;301:142–51.
41. Rutten K, Schiene K, Robens A, Leipelt A, Pasqualon T, Read SJ, et al. Burrowing as a non-reflex behavioural readout for analgesic action in a rat model of sub-chronic knee joint inflammation. Eur J Pain 2014;18:204–12.
42. Galvan A, Raper J, Hu X, Paré JF, Bonaventura J, Richie CT, et al. Ultrastructural localization of DREADDs in monkeys. Eur J Neurosci 2019;50:2801–13.
43. Magnus CJ, Lee PH, Atasoy D, Su HH, Looger LL, Sternson SM. Chemical and genetic engineering of selective ion channel-ligand interactions. Science 2011;333:1292–6.
44. Thompson KJ, Khajehali E, Bradley SJ, Navarrete JS, Huang XP, Slocum S, et al. DREADD agonist 21 is an effective agonist for muscarinic-based DREADDs in vitro and in vivo. ACS Pharmacol Transl Sci 2018;1:61–72.